© 2003 Wiley-Liss, Inc.

Automated Analysis of Morphometric Parameters for Accurate Definition of Erythrocyte Cell Shape

Maria C. Albertini,[1*] Laura Teodori,[2] Elena Piatti,[1] Maria P. Piacentini,[1] Augusto Accorsi,[1] and Marco B. L. Rocchi[3]

[1]Istituto di Chimica Biologica "G. Fornaini", Università degli Studi di Urbino, Urbino, Italy
[2]Unità di Biotecnologie, Sezione di Tossicologia e Scienze Biomediche, ENEA-Casaccia, Roma, Italy
[3]Istituto di Biomatematica, Università degli Studi di Urbino, Urbino, Italy

Received 4 June 2002; Revision Received 12 September 2002; Accepted 28 October 2002

Background: Modification of erythrocyte morphology is clinically important in hematology and medicine. Its detection is routinely performed by subjective microscopic evaluation, which is difficult and strongly dependent on the operator's expertise. We developed an original automated methodology to analyze erythrocyte cell shape modification to support and improve the operator's capability and expedite measurements.
Methods: We used morphometric parameters derived from optical microscope images elaborated with an image processing software (NIH Scion Image) to construct a new application for statistical multivariate discriminant analysis.
Results: For each cell type the elaboration of the morphometric parameters allowed us to develop a chromogenic index, a dimension index, a biconcavity index, and a density profile. The measurements of these indexes were used to construct a statistical methodology that could discriminate among erythrocyte morphologies according to Bessis. When applied casewise, the model effectively differentiated between discocytes, target cells, ovalocytes, macrocytes, and microcytes, with an agreement of 70% between actual and predicted classifications.
Conclusions: The results clearly demonstrated that a set of opportunely selected morphometric parameters derived from optical microscope images and statistically analyzed can effectively discriminate with a high degree of certainty among different shape modifications that red blood cells can undergo in various in vitro and in vivo conditions. This method represents the first attempt to automate the definition of erythrocyte morphology and may have important applications in cases in which the detection of erythrocyte cell shape changes is crucial. Cytometry Part A 52A:12–18, 2003.
© 2003 Wiley-Liss, Inc.

Key terms: erythrocyte morphology; target cells; ovalocytes; macrocytes; microcytes; cup-shaped cells; echinocytes; NIH Scion Image; morphometric parameters; statistical multivariate discriminant analysis; automated analysis

The study of cell shape transformation of human erythrocyte is of great hematologic interest because several clinical conditions are associated with erythrocyte shape changes (1–3). Modifications of cytoskeletal composition and/or organization can alter erythrocytic properties and shapes, which are responsible for the onset of hemolytic damage (4). The red blood cell membrane skeleton mostly determines the shape (discoid), deformability (rheologic properties), and durability (half-life and resistance to shear stress) of the erythrocyte. Erythrocyte aging accompanied by reduced deformability is considered to be among the factors limiting the survival of old erythrocytes. Indeed, the process of reversible erythrocyte shape changes is a property that is limited in aged human erythrocytes (5).

Thus far, the definition of cell shape is routinely performed by subjective microscopic evaluation, which is long, difficult to estimate, and strongly dependent on the operator's expertise (6–10). No attempt of automated analysis has been proposed thus far. In the present study we propose an original application of a statistical model to automatically define erythrocytic cell shape by using suitable morphometric parameters acquired from optical microscope images elaborated with an image processing software (NIH Scion Image). Moreover, we have developed the feasibility of using such processing software to discover as much information as possible on cell shape definition.

Erythrocytes from healthy subjects were incubated with different compounds known to modify the normal discoid cell shape. These treatments allowed us to obtain seven different and peculiar cell morphologies previously described by Bessis (11): discocyte (normal), echinocyte,

*Correspondence to: Dott. Maria C. Albertini, Istituto di Chimica Biologica "G. Fornaini", Via Saffi, 2, 61029 Urbino, Italy.
E-mail: cemetbio@uniurb.it
Published online in Wiley InterScience (www.interscience.wiley.com).
DOI: 10.1002/cyto.a.10019

Table 1
Groupwise Morphometric Data

	CI	DI	BI	DP
$P <$ [a]	0.0001	0.0001	0.0001	0.0001
Discocyte (n = 120)	148.39 (2.87)*	0.25 (0.03)	47.82 (1.15)	4.48 (0.84)*
Target cell (n = 96)	149.70 (2.33)°	0.32 (0.02)°	403.76 (1.42)°	4.78 (0.62)°
Ovalocyte (n = 71)	148.19 (2.56)*	0.37 (0.04)	41.33 (1.69)°	4.54 (0.53)*°
Macrocyte (n = 38)	147.31 (2.98)*	0.33 (0.04)°	42.78 (1.00)	4.19 (0.48)*
Cup-shaped cell (n = 59)	148.85 (4.93)*°	0.27 (0.02)*	40.05 (2.99)°	4.79 (0.97)*°
Echinocyte (n = 22)	153.85 (5.43)^	0.30 (0.06)°*	39.12 (3.39)°	5.61 (2.41)*°^
Microcyte (n = 137)	152.92 (2.18)^	0.21 (0.02)	46.37 (1.27)	5.64 (0.97)^

*Data are presented as mean (standard deviation). BI, biconcavity index; CI, chromogenic index; DI, dimension index; DP, density profile.
[a]*P* values refer to univariate analysis of variance. Groups identified with common symbols in a single column are not significantly different from one another (Dunett's C test).

microcyte, macrocyte, ovalocyte, target cell, and cup-shaped cell. For each cell type, the image processing software allowed us to evaluate a chromogenic index (CI), a dimension index (DI), a biconcavity index (BI), and a density profile (DP). The measurements of these indexes were used for multivariate discriminant analysis by powerful statistical computer programming to achieve a reliable and objective statistical method that can discriminate among the seven erythrocytic morphologies as classified by Bessis.

MATERIALS AND METHODS

Erythrocyte Treatments

Human erythrocytes were collected by venipuncture from healthy adult volunteer donors into sterile tubes containing heparin as the anticoagulant. Whole blood was diluted with 1:2 (v/v) RPMI medium (product no. R-8755, Sigma, St. Louis, MO) and incubated at 37°C for 2 h under different conditions: no addition (controls) and discrete additions of 10 mM of deoxyglucose, 1 mM of ethylene glycol-bis (β-aminoethyl ether)-N,N,N′,N′-tetraacetic acid (EGTA), 1 mM of neomycin, and 500 ng/ml of A23187.

Morphologic Evaluations

Erythrocyte images acquired by a phase-contrast Nikon Optiphot microscope coupled with a Hamamatsu 5985 camera were processed by NIH Scion Image 1.61 on a Macintosh 6100/66 computer to estimate shape parameters. Seven different erythrocyte morphologies (groups) were chosen by subjective shape assessment according to the Bessis's classification (11). The shapes were discocyte, echinocyte, microcyte, macrocyte, ovalocyte, target cell, and cup-shaped cell. We used the program set scale option to perform spatial calibration, so that the results were represented in inch calibrated units (for area measurements) and optical density calibrated units (for peak evaluation). The program rectangular option was selected for every erythrocyte to be measured because it allows parameter estimation. We selected the following parameters to measure by the image processing software as the most representative of cell shape: CI, DI, BI, and DP. We derived these indexes from the mean gray density of the selection, the area of the selection, the standard deviations of CI values, and the integrated mean density parameters, respectively.

Statistical Analysis

The CI, DI, BI, and DP were calculated from 543 erythrocytes because this number is very representative for the statistics applied. The numbers of cells in each group are reported in Table 1. After measuring the DI, CI, BI, and DP of each erythrocyte, we calculated the arithmetic mean and the standard deviation of each morphometric parameter for each morphologic type (group). In addition, an exploratory analysis of variance followed by Dunnett's C test for multiple comparisons were performed to identify significant differences among the seven morphologic types (groups). Thus, we built a discriminant model (12) with DI, CI, BI, and DP as predictor variables. The hypothesis of equal covariance matrices for each group was tested by Box's test. The discriminant analysis we are proposing allowed us to calculate the canonical discriminant functions, defined as independent linear combinations of predictor variables that maximize the distances across the mean of each group. Because the number of canonical discriminant functions is equal to the minimum between the number of groups minus one and the number of predictor variables, our discriminant analysis provided four discriminant functions. Further, the coefficients for each predictor variable were calculated to build a classification functional equation for each of the seven groups. The resultant equations, also called Fisher linear discriminant functions or, simply, classification functions (CFs), were used to assign each erythrocyte to one of the seven groups. A casewise testing was performed as follows: for each erythrocyte, the value of each of the four predictor variables was inserted into each CF; an erythrocyte was predicted as belonging to the group in which the value of its CF was the largest. The predicted assignments were then compared with the actual classification of each erythrocyte. The percentage of agreement and Cohen's coefficient of agreement (13) were then calculated, and the results were evaluated according to the scale of Landis and Koch (14) and the test of Fleiss et al. (15). To avoid

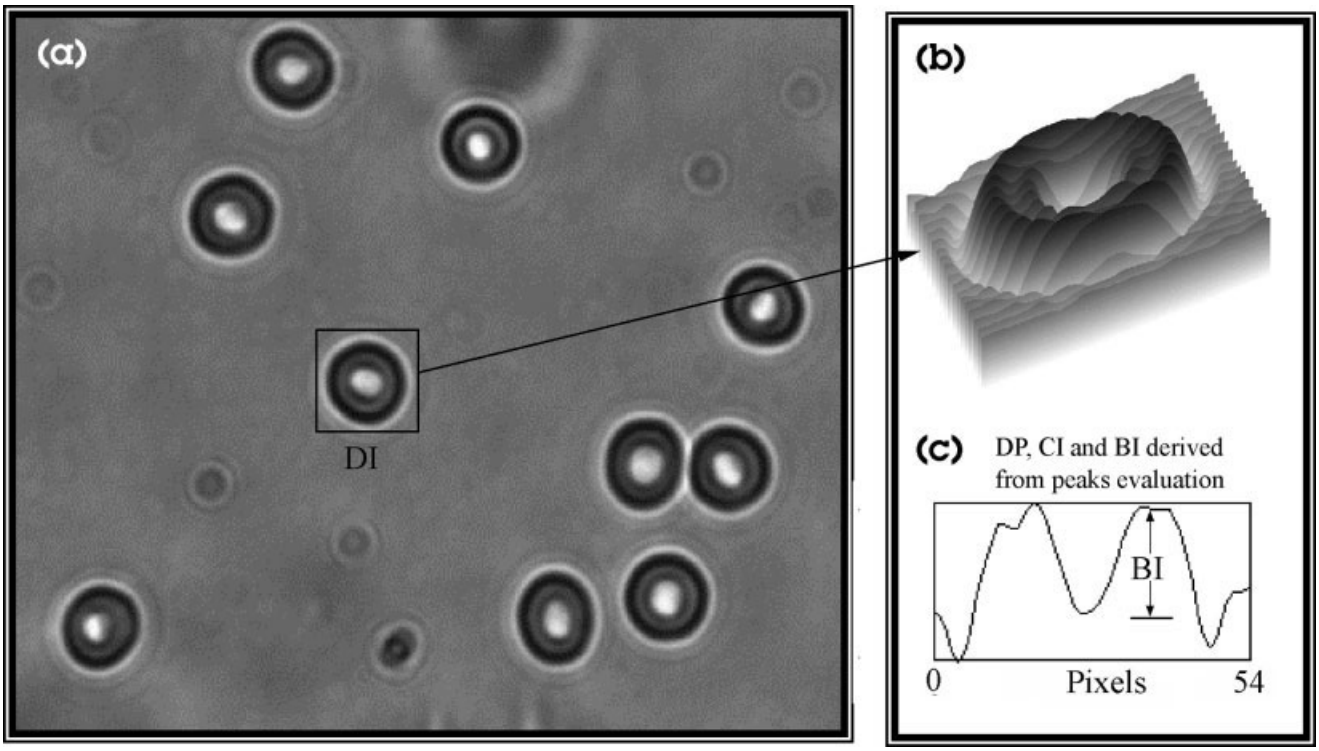

FIG. 1. Erythrocyte image processing by NIH Scion Image software. One cell on the microscope slide image (**a**), acquired as described in Materials and Methods, is selected by the rectangular tool. This permits one to obtain the tridimensional surface plot (**b**) and the plot profile (**c**) needed to define cell morphology (11) and morphometric values. The option dialog box allows one to specify which measurement is recorded by the measure and analyze particle command. The selected measurements were area (area of the selection in pixels; DI, dimension index), mean density (average gray value within the selection; CI, chromogenic index), standard deviation (of the gray values used to generate the mean gray value; BI, biconcavity index), and integrated density (sum of the gray values in the selection, with background subtracted; DP, density profile).

overestimating the agreement percentage between observed and predicted classifications, a cross-validation study was performed, in which each erythrocyte was classified by the CFs obtained from all the other erythrocytes (according to the jackknife method of estimation). Moreover, sensitivity and specificity were calculated separately for each morphometric group from casewise testing and cross-validation analysis. A diagram of the erythrocytes (with the centroids of the seven groups) in the bidimensional space, defined by the first and second canonical discriminant functions, was also plotted. Statistical significance was fixed at 0.05. All statistical analyses were performed with SSPS 9.0.

RESULTS

Human erythrocytes were collected, diluted, and incubated with different compounds (see the Introduction and Materials and Methods) to induce the formation of abnormal cell shapes.

Subsequent microscopic observations led us to group the observed shapes into the seven different morphologies described by Bessis (11): discocytes (normal), echinocytes, microcytes, macrocytes, ovalocytes, target cell, and cup-shaped cell. With the image analysis program Scion Image, the cell surface plot was then obtained for each examined cell (Fig. 1). We selected, as the most representative of cell shape, the CI, DI, BI, and DP. We found these parameters the most suitable for defining cell shape because CI and DP are representative of erythrocytic morphology (e.g., discocytes show a central pallor, and target cells show a central gray color), DI depends on the cell shape (e.g., microcytes are smaller than discocytes), and BI is representative of the biconcavity of the cell (e.g., discocytes have a great BI value for the larger standard deviation values obtained from the differences in gray density between the central pallor and the remainder of the cell).

Figure 2 shows the representative measurements of the seven erythrocytic morphologies.

Statistical analysis was performed on the data collected from 543 erythrocytes subdivided into seven groups (11).

Table 1 shows the data grouped on the basis of the four measured morphometric variables (CI, DI, BI, and DP) and on the basis of their assignment to the Bessis classification group. Table 1 also shows results from analysis of variance and Dunnett's C test for multiple comparisons. Table 2 shows the four canonical discriminant functions. The discriminant analysis showed that the first and second canonical discriminant functions cumulatively accounted for 96.4% of the variance. Thus, the choice of just the first and second discriminant functions correctly illustrated the model and allowed us to present the data bidimensionally.

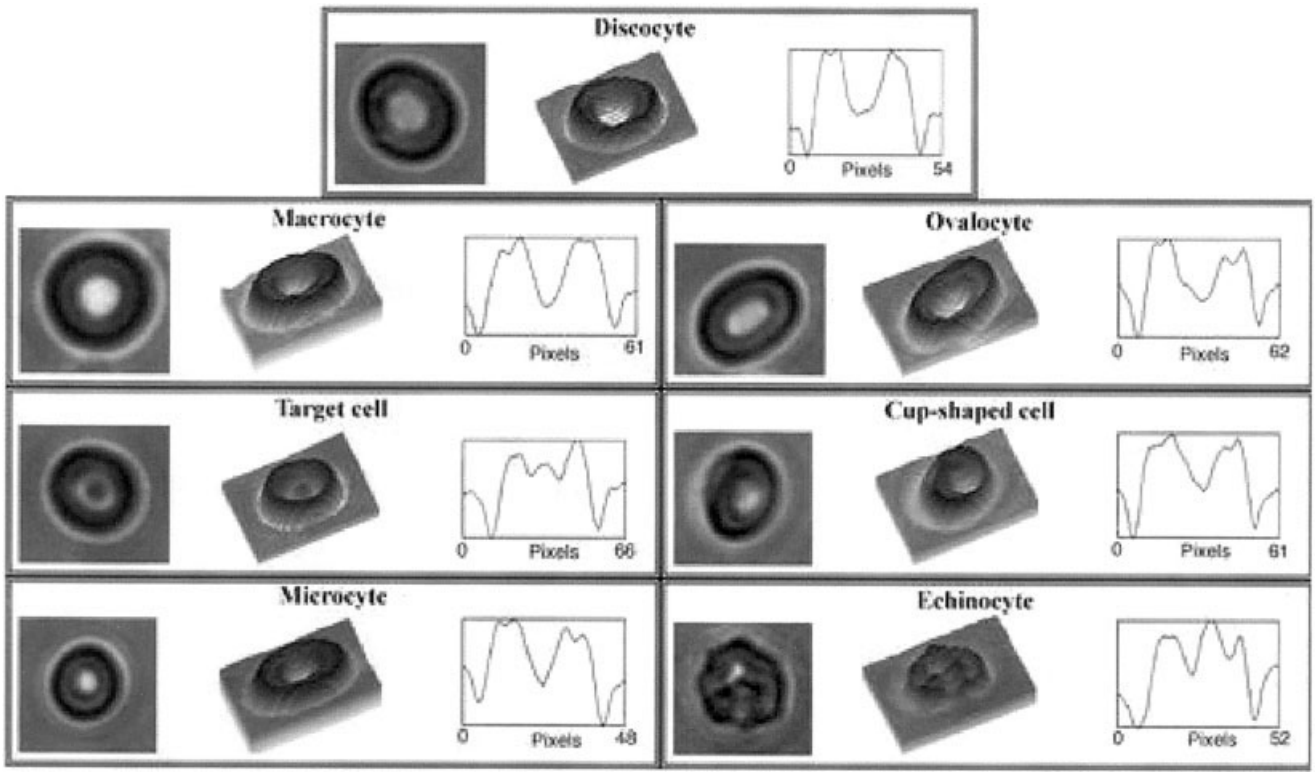

FIG. 2. Morphologic definition and morphometric measurements of selected cells. Seven different morphologies were identified according to Bessis's classification (11).

Figure 3 displays all 543 erythrocytes in the bidimensional space defined by the first and second canonical discriminant functions and the centroid of each group. It clearly shows the discriminant power of the model (details are reported in the Discussion).

Table 3 clarifies the links between the canonical functions and the original variables by presenting the structure matrix of the model, where the correlation between each variable and any canonical function is reported. The data indicate that the first canonical function depends chiefly on BI and DI, whereas the second canonical function correlates with BI and CI (as derived from the highest absolute values of correlation).

The coefficients of the Fisher linear classification functions are shown in Table 4. These coefficients were used to build the seven classification equations corresponding to the seven morphologic groups (11) and have the following form:

Table 2
Summary of Canonical Discriminant Functions

Function	Eigenvalue	Variance (%)	Cumulative variance (%)	Canonical correlation
1	6.119	80.0	80.0	0.927
2	1.255	16.4	96.4	0.746
3	0.274	3.5	99.9	0.464
4	0.004	0.1	100.0	0.063

$$CF = CI \cdot Coef_{CI} + DI \cdot Coef_{DI} + BI \cdot Coef_{BI} + DP \cdot Coef_{DP} + Constant$$

where CF is the classification function of the group, CI is the erythrocytic chromogenic index, $Coef_{CI}$ is the group classification coefficient for CI, DI is the erythrocytic dimension index, $Coef_{DI}$ is group classification coefficient for DI, BI is the erythrocytic biconcavity index, $Coef_{BI}$ is the group classification coefficient for BI, DP is the erythrocytic density profile, $Coef_{DP}$ is the group classification coefficient for DP, and Constant is the group classification constant.

To obtain the classification of an erythrocyte according to this model, its measured variables have to be substituted into the seven classification equations having the classification coefficients shown in Table 4; the group with the largest CF value is the most probable classification for that erythrocyte. The Appendix shows an application to actual data.

The summary results of the casewise testing of the original set of 543 erythrocytes with the Fisher CFs are reported in Table 5. The comparison between predicted and observed classification shows an agreement of 74.2%, ranging from a minimum of 45.5% (echinocytes) to a maximum of 90.0% (discocytes). Moreover, Cohen's coefficient of agreement equalled 0.69 (95% confidence interval, 0.65–0.73; test of Fleiss et al., $Z = 35.93$, $P < 0.0001$);

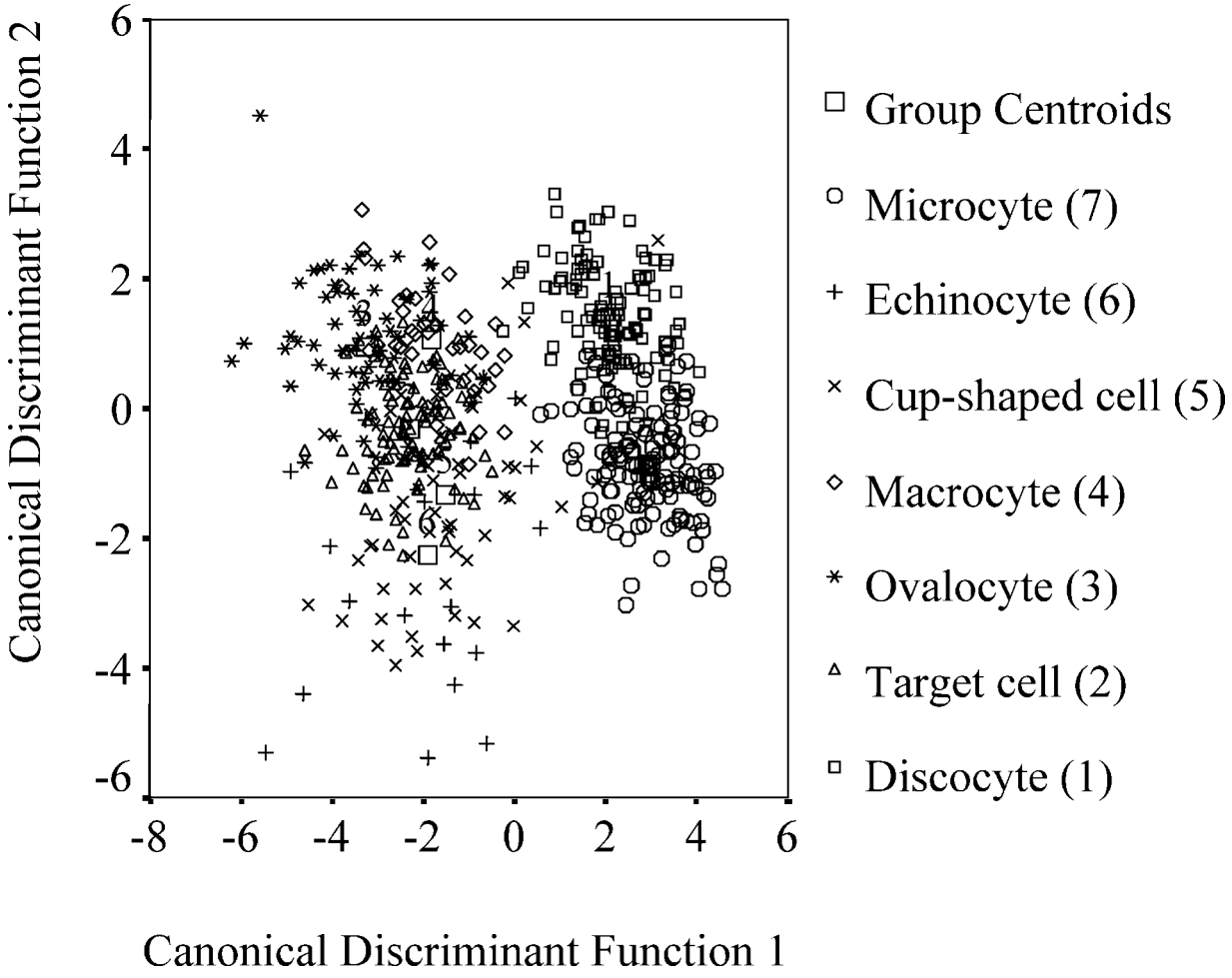

FIG. 3. Erythrocytes displayed in the space of the first and second canonical discriminant functions.

this agreement degree can be classified as "substantial" according to the scale of Landis and Koch (that is <0% = poor; 0%-20% = slight; 21%-40% = fair; 41%-60% = moderate; 61%-80% = substantial; 81%-100% = almost perfect). This scale is widely applied also in clinical contexts. Table 5 also shows the classification results of a cross-validation study, in which each erythrocyte was classified from the CFs obtained from all other erythrocytes. The agreement equalled 72.2%.

Table 3
*Structure Matrix of the Model**

Variables[a]	Function 1	Function 2	Function 3	Function 4
BI	0.691	0.680	0.224	0.097
DI	−0.657	0.427	0.618	0.072
DP	0.109	−0.378	0.424	0.816
CI	0.137	−0.460	0.611	−0.630

*Values indicate correlation between each variable and any discriminant function.

[a]BI, biconcavity index; CI, chromogenic index; DI, dimension index; DP, density profile.

Table 6 shows the sensitivity and specificity of the proposed discriminant model obtained from casewise testing and cross-validation analysis for each kind of morphology.

DISCUSSION

We have proposed a new, automated, cell morphology evaluation that uses statistical analysis of cell morphomet-

Table 4
*Fisher Linear Classification Function Coefficients**

	CI	DI	BI	DP	Constant
Discocyte	17.823	170.392	20.965	8.969	−1866.847
Target cell	17.738	243.548	18.557	9.048	−1769.872
Ovalocyte	17.555	293.419	18.719	8.573	−1763.522
Macrocyte	17.513	248.187	19.191	8.298	−1760.209
Cup-shaped cell	17.562	188.614	18.273	9.198	−1729.021
Echinocyte	18.187	214.47	18.107	10.201	−1816.056
Microcyte	18.335	128.53	20.595	10.574	−1924.985

*BI, biconcavity index; CI, chromogenic index; DI, dimension index; DP, density profile.

Table 5
Classification Results (Actual Versus Predicted) for Casewise Testing and Cross-Validation Analysis (Jackknife Method)

	Predicted							
Actual	Discocyte	Target cell	Ovalocyte	Macrocyte	Cup-shaped cell	Echinocyte	Microcyte	Total
Casewise testing								
Discocyte	108 (90.0%)	0 (0%)	0 (0%)	1 (0.8%)	0 (0%)	0 (0%)	11 (9.2%)	120 (100.0%)
Target cell	0 (0%)	57 (59.4%)	10 (10.4%)	16 (16.7%)	8 (8.3%)	5 (5.2%)	0 (0%)	96 (100.0%)
Ovalocyte	0 (0%)	8 (11.3%)	48 (67.6%)	12 (16.9%)	3 (4.2%)	0 (0%)	0 (0%)	71 (100.0%)
Macrocyte	0 (0%)	2 (5.3%)	10 (26.3%)	23 (60.5%)	3 (7.9%)	0 (0%)	0 (0%)	38 (100.0%)
Cup-shaped cell	3 (5.1%)	4 (6.8%)	0 (0%)	3 (5.1%)	34 (57.6%)	13 (22.0%)	2 (3.4%)	59 (100.0%)
Echinocyte	0 (0%)	2 (9.1%)	2 (9.1%)	2 (9.1%)	6 (27.3%)	10 (45.5%)	0 (0%)	22 (100.0%)
Microcyte	14 (10.2%)	0 (0%)	0 (0%)	0 (0%)	0 (0%)	0 (0%)	123 (89.8%)	137 (100.0%)
Cross-validation analysis								
Discocyte	108 (90.0%)	0 (0%)	0 (0%)	1 (0.8%)	0 (0%)	0 (0%)	11 (9.2%)	120 (100.0%)
Target cell	0 (0%)	56 (58.3%)	10 (10.4%)	16 (16.7%)	9 (9.4%)	5 (5.2%)	0 (0%)	96 (100.0%)
Ovalocyte	0 (0%)	8 (11.3%)	48 (67.6%)	12 (16.9%)	3 (4.2%)	0 (0%)	0 (0%)	71 (100.0%)
Macrocyte	0 (0%)	2 (5.3%)	10 (26.3%)	23 (60.5%)	3 (7.9%)	0 (0%)	0 (0%)	38 (100.0%)
Cup-shaped cell	3 (5.1%)	5 (8.5%)	0 (0%)	5 (8.5%)	29 (49.2%)	14 (23.7%)	3 (5.1%)	59 (100.0%)
Echinocyte	0 (0%)	3 (13.6%)	2 (9.1%)	2 (9.1%)	7 (31.8%)	7 (31.8%)	1 (4.5%)	22 (100.0%)
Microcyte	16 (11.7%)	0 (0%)	0 (0%)	0 (0%)	0 (0%)	0 (0%)	121 (88.3%)	137 (100.0%)

ric parameters acquired by microscope image measurements. The availability of computers and powerful statistical software has expanded the accessibility and inexpensiveness of sophisticated statistical analyses including those that use multiple predictor variables (multivariate analysis). From this wide array of multivariate analyses, multiple regression, logistic regression, and cluster analysis were rejected. Multiple linear regression usually requires that the outcome variable be measured on an interval scale; logistic regression requires a dichotomous categoric outcome variable; and cluster analysis classifies groups with no a priori knowledge of the number of groups or group membership (16). Thus, discriminant analysis seemed the most suitable for the purposes of our study. We wanted to assess whether or not a set of variables could discriminate between at least two populations. The discriminant analysis identifies the linear combinations of quantitative predictor variables that best characterize the differences between groups. This procedure (performed on a training set) estimates the coefficients for each variable, and the resulting functions provide an allocation rule that can be used to classify new cases.

Table 6
Summary Report of Sensitivity and Specificity Obtained for Each Kind of Morphology From Casewise Testing and Cross-Validation Analysis

	Casewise testing		Cross-validation	
Morphology	Sensitivity	Specificity	Sensitivity	Specificity
Discocyte	0.90	0.96	0.90	0.96
Target cell	0.59	0.96	0.58	0.96
Ovalocyte	0.68	0.95	0.68	0.95
Macrocyte	0.61	0.93	0.61	0.93
Cup-shaped cell	0.58	0.96	0.49	0.95
Echinocyte	0.45	0.97	0.32	0.96
Microcyte	0.90	0.97	0.88	0.96

By using morphometric parameters from seven different erythrocytic cell shape morphologies, we could construct seven CFs. When applied casewise, the allocation rule effectively differentiated between discocytes, target cells, ovalocytes, macrocytes, and microcytes, with an agreement of 70% between actual and predicted classifications. When the erythrocytes were plotted in the space defined by the first two canonical discriminant functions, two clusters were evident: the first cluster consisted of target cells, ovalocytes, and macrocytes, which were similar according to the first canonical function; the second consisted of discocytes and microcytes. In contrast, echinocytes and cup-shaped cells were dispersed throughout the plot and separated from both clusters (Fig. 3). In addition, microcytes and discocytes shared first canonical function values but not second canonical function values, probably because they had the same cellular shape but different dimensions (microcytes are smaller than discocytes; Fig. 3).

The advantages of using a method based on NIH Scion Image (rather than other, more sophisticated software) are its easy access (it can be downloaded free from Scion Corporation) (17), its ease of use, and its considerable degree of sensitivity and specificity with regard to definition of erythrocytic morphology (Table 6). Nevertheless, the proposed statistical model can be applied successfully to data obtained from other, more sophisticated image analysis software. Indeed, more accurate estimations of the morphometric indexes may allow the construction of a discriminating model even more valid than ours.

In some of our current studies, we are successfully using this method as an analytical tool to detect biological effects in toxicologic studies, thus using the erythrocytes as biosensors.

In conclusion, because recognizing alterations in normal erythrocytic shape is important for experimental and clinical purposes (18,19), we believe that our method

provides a useful tool to discriminate erythrocytic cell shape changes in an objective way and with a high degree of certainty, thus providing a valuable support to the morphologic examination.

APPENDIX: EXAMPLE APPLICATION OF THE DISCRIMINANT MODEL TO ACTUAL ERYTHROCYTIC DATA

Let consider an erythrocyte for which the following variables were recorded:

$$CI = 150.98$$

$$DI = 0.22$$

$$BI = 46.29$$

$$DP = 7.46$$

This erythrocyte was classified a priori as a microcyte by an expert operator.

Now, these values must be inserted into each CF, having the form:

$$CF = CI \cdot Coef_{CI} + DI \cdot Coef_{DI} + BI \cdot Coef_{BI} + DP \cdot Coef_{DP} + Constant$$

built with coefficients and constants listed in Table 4.

The following seven equations result:

$$CF_{discocyte} = 150.98 \cdot 17.823 + 0.22 \cdot 170.392 + 46.29 \times 20.965 + 7.46 \cdot 8.969 - 1866.847 = 1898.934$$

$$CF_{target\ cell} = 150.98 \cdot 17.738 + 0.22 \cdot 243.548 + 46.29 \times 18.557 + 7.46 \cdot 9.048 - 1769.872 = 1888.293$$

$$CF_{ovalocyte} = 150.98 \cdot 17.555 + 0.22 \cdot 293.419 + 46.29 \times 18.719 + 7.46 \cdot 8.573 - 1763.522 = 1881.941$$

$$CF_{macrocyte} = 150.98 \cdot 17.513 + 0.22 \cdot 248.187 + 46.29 \times 19.191 + 7.46 \cdot 8.298 - 1760.209 = 1888.759$$

$$CF_{cup\text{-}shaped\ cell} = 150.98 \cdot 17.562 + 0.22 \cdot 188.614 + 46.29 \times 18.273 + 7.46 \cdot 9.198 - 1729.021 = 1878.459$$

$$CF_{echinocyte} = 150.98 \cdot 18.187 + 0.22 \cdot 214.470 + 46.29 \times 18.107 + 7.46 \cdot 10.201 - 1816.056 = 1891.273$$

$$CF_{microcyte} = 150.98 \cdot 18.335 + 0.22 \cdot 128.530 + 46.29 \times 20.595 + 7.46 \cdot 10.574 - 1924.985 = 1903.734$$

Because the CF for microcytes yielded the highest value (1903.734), the predicted classification agrees with the actual one.

LITERATURE CITED

1. Turchetti V, De Matteis C, Leoncini F, Trabalzini L, Guerrini M, Forconi S. Variations of erythrocyte morphology in different pathologies. Clin Hemorheol Microcirc 1997;17:209–215.
2. Bossi D, Russo M. Hemolytic anemias due to disorders of red cell membrane skeleton. Mol Aspects Med 1996;17:171–188.
3. Agroyannis B, Dalamangas A, Tzanatos H, Soubassi L, Fourtounas C, Kopelias I, Bovoleti O, Bosiolis V, Koutsikos D. Alterations in echinocyte transformation and erythrocyte sedimentation rate during hemodialysis. Artif Organs 1997;21:327–330.
4. Nakao M, Jinbu Y, Sato S, Ishigami Y, Nakato T, Ito Ueno E, Wake K. Structure and function of red cell cytoskeleton. Biomed Biochim Acta 1987;46:S5–S9.
5. Marikovsky Y. The cytoskeleton in ATP-depleted erythrocytes: the effect of shape transformation. Mech Ageing Dev 1996;86:137–144.
6. Thimon L, Peypoux F, Exbrayat JM, Michel G. Effect of iturin A, a lipopeptide from *Bacillus subtilis* on morphology and ultrastructure of human erythrocytes. Cytobios 1994;79:69–83.
7. Yawata Y, Kanzaki A, Inoue T, Ata K, Wada H, Okamoto N, Higo I, Yawata A, Sugihara T, Yamada O. Red cell membrane disorders in the Japanese population: clinical, biochemical, electron microscopic, and genetic studies. Int J Hematol 1994;60:23–38.
8. Grebe R, Schmid Schonbein H. Tangent counting for objective assessment of erythrocyte shape changes. Biorheology 1985;22:455–469.
9. Turchetti V, Leoncini F, De Matteis C, Trabalzini L, Guerrini M, Forconi S. Evaluation of erythrocyte morphology as deformability index in patients suffering from vascular diseases, with or without diabetes mellitus: correlation with blood viscosity and intra-erythrocytic calcium. Clin Hemorheol Microcirc 1998;18:141–149.
10. Zipursky A, Brown E, Palko J, Browna EJ. The erythrocyte differential count in newborn infants. Am J Pediatr Hematol Oncol 1983;5:45–51.
11. Bessis M. Cellules du sang normal et pathologiques. Paris: Masson et Cie; 1972.
12. Anderson TW. An introduction to multivariate statistical analysis. New York: John Wiley & Sons; 1984.
13. Cohen J. A coefficient of agreement for nominal scales. Educ Psychol Meas 1960;20:37–46.
14. Landis RJ, Koch GG. The measurement of observer agreement for categorical data. Biometrics 1977;33:159–174.
15. Fleiss JL, Cohen J, Everitt BS. Large sample standard errors of kappa and weighted kappa. Psycol Bull 1969;72:323–327.
16. Eldibany M, Totonchi K, Joseph N, Rhone D. Usefulness of certain red blood cell indices in diagnosis and differentiating thalassemia trait from iron-deficiency anemia. Am J Clin Pathol 1999;111:676–682.
17. Scion Corporation. Scion products. Frederick, MD: Scion Corporation. Updated 1 October 2002. Available from: http://scioncorp.com/frames/fr_scion_products.htm
18. Hung TC, Pham S, Steed DL, Webster MW, Butter DB. Alterations in erythrocyte rheology in patients with severe peripheral vascular disease. Angiology 1991;42:210–217.
19. Ayala S, Besson I, Aymerich M, Berga L, Vives Corrons JL. Abnormal changes in erythrocyte membrane proteins in hereditary spherocytosis and their relation to clinical and biological aspects of the disease. Med Clin Barc 1995;105:45–49.